Journal of Cultural Heritage 61 (2023) 23–31

Contents lists available at ScienceDirect

Journal of Cultural Heritage

journal homepage: www.elsevier.com/locate/culher

Original article

A numerical model for predicting the time for crack initiation in wood panel paintings under low-cycle environmentally induced fatigue

R. Zhang [a,*], A.C. Taylor [a], M.N. Charalambides [a], D.S. Balint [a], C.R.T. Young [b], D. Barbera [c], N. Blades [d]

[a] Department of Mechanical Engineering, Imperial College London, South Kensington Campus, London SW7 2AZ, UK
[b] Kelvin Centre for Conservation and Cultural Heritage Research, Glasgow University, Kelvin Hall, Glasgow G3 8AW, UK
[c] College of Engineering and Physical Sciences, University of Glasgow, Glasgow G12 8QQ UK
[d] Conservation Science, National Trust, 20 Grosvenor Gardens, London SW1W 0DH, UK

ARTICLE INFO

Article history:
Received 4 December 2022
Accepted 22 February 2023

Keywords:
Paintings conservation
Environmental low-cycle fatigue
Interfacial crack
Irreversible cohesive zone model
Through-thickness (channelling) crack

ABSTRACT

Determining the storage and display conditions for historical panel (wood) paintings requires a balance between ensuring the painting's preservation whilst also considering the energy consumption associated with climate control. The latter has become very important due to the need to lower the carbon footprint of museums and historical houses. In order to address this need, we have developed numerical models based on finite element analysis to simulate the initiation of two types of potential damage in panel paintings, namely interfacial and channelling cracks in the oil paint layer, under cyclically varying relative humidity. These models are based on our case study at Knole House (National Trust), Kent. Using known data for the past environment in which the paintings within the Brown Gallery at Knole House have been exposed, the ambient RH variation was approximated by three cycles, i.e., annual, biannual, and monthly varying cycles. Four RH cases, one containing all three cycles and each of the other three cases containing just two of the three cycles, were applied as boundary conditions to simplified geometries of the panel paintings in an effort to investigate the effects of the frequency and the amplitude of the variation on the possibility of cracking in the painting. The models need several material parameters as input which are not all available. Therefore, the study also includes some parametric studies to determine possible variations in the crack initiation. According to the model predictions, the channelling crack initiates slightly earlier than the interfacial crack. The crack initiation time in an uncontrolled environment (containing all three RH cycles) predicted by the model is approximately 120 years which empirically is a realistic estimate. Furthermore, the annual RH cycle (high amplitude and low frequency) has the most significant effect on the crack initiation. By removing the annual variation from the RH cycle, the initiation of both channelling and interfacial cracks can be postponed significantly, from approximately 120 years to over 400 years.

1. Introduction

Wood has served as a support material for paintings in Europe for centuries before it was gradually replaced by canvas in the sixteenth century. Within cultural heritage, painted wooden objects including panel paintings respond to fluctuations in relative humidity (RH) and to a lesser extent, temperature. Thus, the environment in which they are stored, displayed, and transported is an important factor to consider when establishing environmental protocols for their preservation. Panel paintings have a complex multi-layer structure which, in the Sixteenth and Seventeenth Century Northern tradition, is typically composed of a wood (usually oak) support sized with animal glue, a preparatory ground layer of chalk in animal glue, and finally paint layers (pigments in a drying oil). All these materials are sensitive to changes in relative humidity. They contract when they lose moisture and expand when they absorb moisture. This process generates a strain mismatch due to the different expansion coefficients of the materials and the resulting stresses can lead to damage in the form of cracking within the panel paintings [1].

* Corresponding author.
E-mail address: r.zhang13@imperial.ac.uk (R. Zhang).

https://doi.org/10.1016/j.culher.2023.02.007

To reduce the effect of the fluctuating relative humidity, vulnerable panel paintings are kept in controlled or semi-controlled environments, with additional preventive measures including glazing and back boards. However, the challenge to meet the commitment to reduce the carbon footprint while at the same time achieve the best preservation of collections, is ever more pertinent. Having a better understanding of the amplitude, frequency, and number of cycles of relative humidity fluctuation which cause fracture as well as the mechanisms which lead to damage, will help in the development of sustainable environmental control protocols.

Before the 1990s, the environmental control protocols were designed based on the technical capabilities of climate control systems and to a large extent on empirical evidence. This resulted in the most widely used museum environmental specification of 21 or 22 ± 1 °C in temperature and 50 ± 5% in RH for mixed collections [2,3].

Since the 1990s, as more material testing was employed in the field of conservation, data is available on the dimensional response of wood, paint, and other painting layers to environmental fluctuations, on which to base environmental specifications. Some authors consider a RH variation of 50 ± 10% as safe for wood panel paintings [3,4], whereas RH variations over 20% dramatically increase the risk of painting damage. However, semi-controlled environments which contain panel paintings, e.g., churches and historical houses, must take a more pragmatic approach. Some argue that institutions that presently adhere to tighter controls will need to adopt a more relaxed but evidence-based "safe" environmental specifications which can reduce energy consumption and carbon footprint significantly [3,5,6]. More institutions and museums are adopting evidence-based environmental specifications because research has shown that even a slight relaxation of the specification can reduce energy consumption and carbon footprint significantly [3,6,7]. For instance, the Smithsonian Institution was able to cut energy costs by 17% by relaxing the controlled RH range from ±5% to ±8% [3].

A 'safe' RH range has been suggested based on mechanical tests on undamaged, new materials [4]. In reality each layer in a panel painting has mechanical properties different to the equivalent new, unaged materials because of its age and long environmental history. However, it is nearly impossible to conduct a comprehensive mechanical characterisation study on naturally aged samples because the ageing process of paints occurs over an extremely long period. For example, the properties of lead white oil paint change rapidly in the first fourteen years but are still changing after thirty years [5,7]. Computational finite element (FE) models have a great potential in optimising the environmental specification for panel paintings; such models enable parametric studies, highlighting the critical material parameters and the effect of uncertainties in these values on the stress and strain in the painting in an efficient manner. However, it is noted that some mechanical testing is still needed to obtain the baseline figures for the material parameters used as input in the FE models.

Damage, especially cracking in the paint layers of oil paintings has been studied previously, though not extensively. Fracture of the wooden support usually occurs due to restraint from battens, frame elements and internal stresses within the support (wood is a composite) with changes in moisture content. Such cracking in the wood can lead to fractures of the paint. Crack development can also occur due to the stress transfer from the intact wood substrate to the more fragile layers [6,8]. This research focuses on the latter mechanism. Wood is most moisture responsive across the grain, especially in the tangential cut direction, and this often leads to warping of the panel. A panel that is painted on one side only will often warp due to differential diffusion of moisture. However, raised cracks are seen on panels that have not warped and the reason for this phenomenon is thought to be a strain mismatch between the upper layers and the wood which is contracting and expanding differentially across the grain under varying RH which leads to a set of parallel cracks (shown in Supplementary Fig. 1) [9]. A study by Krzemień et al. [10] shows that if a new panel painting is situated in a building with an uncontrolled climate, the historical crack pattern would fully develop and stabilise within several years.

Because the materials in the wood panel swell and shrink while gaining and losing moisture, panel paintings are subjected to a cyclic load when kept in a semi or uncontrolled environment. This continual cycling over tens to hundreds of years may lead to fatigue as a possible cause of crack initiation and propagation [11–15]. Bosco et al. [14,15] studied RH-induced cracks in an oil paint layer, but this did not take into consideration the effect of varying RH. Roe and Siegmund [16] proposed an irreversible cohesive zone (ICZ) model to enable the FE simulation of low cyclic fatigue. Tantideeravit et al. [11] and Wood et al. [12] used Roe and Siegmund's ICZ model to predict the initiation time of interfacial and channelling cracks using 2-dimentional models for modern paintings that have some layers executed in alkyd paint. More recently, Zhang et al. [13] extended the application of the ICZ to 3-dimensional models for alkyd paintings and proposed a method for predicting the initiation time and crack growth rate of the two types of crack.

Jaskierny [17] performed a semi-quantitative study on forty-four seventeenth century oak panel paintings displayed in the Brown Gallery at Knole House (National Trust), England. This collection is unique in that the panels were commissioned for the house and have remained *in situ* for over four hundred years. This allowed for the classification and measurement of the cracking and delamination present in the pictorial layers including crack length, number of cracks, and the extent of crack networks. The study identified three main types of cracks: (i) interfacial cracks between two of the layers in the paintings, (ii) channelling (through-thickness) cracks within the paint and/or other layers, which extend to/from the layer-substrate (wood) interface, and (iii) the cracks caused by the splits in the wood substrate. As stated earlier, the latter type of crack will not be considered in this study.

The research presented here aims, for the first time, to identify the effect of the magnitude and frequency of RH fluctuation on the initiation and propagation of both channelling and interfacial cracks in the panel paintings at Knole House. Finite element models are employed to simulate the environmentally induced fatigue, using RH data which were measured and extrapolated at the Brown Gallery, Knole House (National Trust), England [18]. These paintings gave a very interesting case study for investigating the effect of changing environment on crack initiation and propagation in the paint layers. This is because the environmental history (since 1600s) of the display and storage conditions has already been reconstructed for the period 1605 – 2015 for this research by Wood et al. [18]. This was achieved by establishing a relationship between the temperature in the Brown Gallery and the Hadley Centre Central England Temperature dataset. The recorded data from inside the Brown Gallery and outside Knole House showed that the inside conditions closely followed the outside conditions with a slight offset in relative humidity. This enabled an environmental profile of 400 years to be built for these paintings [18]. Using technical examination of the paintings to identify the constituent layers and experimental data as well as literature values to obtain mechanical properties of the materials in the layers, the FE model has been used to predict the time to crack initiation and identify which type of crack is likely to appear first. The model can be of great help towards effective management of collections environments. In the long term, it may help to reduce energy use and carbon emissions while maintaining high standards of collection care.

2. Research aim

This research provides a method to model the effective cyclic stress induced by humidity fluctuations in wood panel paintings. With this model, it is possible to study the impact of the environment on the formation of crack damage in historical wood panel paintings. Furthermore, the model can be used to help optimise the display/storage conditions of paintings while maintaining the goal of lowering energy consumption.

3. Methodology

As stated above, the initiation of two possible types of cracks, i.e., a channelling crack and an interfacial crack, in the oil paint layers of the wood panel portraits in the Brown Gallery under varying relative humidity was investigated using finite element analysis (FEA). The oil paint layer was chosen as the layer of interest because during the ageing process, the pigmented linseed oil paint is reported to be the most fragile part in the whole painting [5]. Due to the long history of the paintings, all the four layers (panel, rabbit skin glue (RSG), chalk in RSG and oil paint) are assumed to be "fully aged" so that no further changes take place in their mechanical properties. This ageing is due to the crosslinking and chain scission that has taken place at the molecular level [19] of the drying oil and the animal glue [20]. Because of this, as well as the approximately linear behaviour of wood [21,22], all the materials were simulated using linear elastic models (see Section 3.1). The models of the panel painting were all 2D (plane strain) and were subjected to a cyclically changing RH for the equivalent of 410 years (1605 – 2015), which is the whole length of the extrapolated environmental profile [18] (more details in Section 3.3). The initiation of the cracks under the relative humidity induced cyclic load was simulated using an irreversible cohesive zone model (ICZM) [11,13], described in Section 3.2.

3.1. Material parameters

To perform finite element analysis on the panel paintings, a representative geometry and the properties of each layer need to be obtained. Panel paintings studied in this project are simplified as a composite material consisting of four layers from top to bottom, pigmented oil paint, chalk ground, rabbit skin glue (RSG) and panel made from Baltic oak, as shown in the typical cross section in Fig. 1. The quoted thicknesses of the oil paint layer, chalk ground layer, RSG layer and panel are the averages of direct measurements with microscopy of cross sections from the paintings. The changing climate and local soil conditions result in non-uniform growth-ring width from season to season and year to year within an oak tree. Thus, the width of earlywood (spring) and latewood (summer) are not uniform throughout the life of the tree even for Baltic oak. In this study, typical values of the width of European oak early wood and late wood were obtained from literature as 0.61 mm and 0.42 mm, respectively [23].

It is not possible to perform mechanical tests to obtain the required material parameters for modelling without damaging the panel paintings. Therefore, mechanical tests were performed on freshly prepared RSG and chalk ground specimens. It is also difficult to experimentally obtain the mechanical properties of the oil paint and wood panel because the linseed-oil-based paint takes decades to dry naturally, artificially aged samples on wood are complex to prepare [7] and a 400-year-old oak specimen is very rare. In this study, the properties of the oil paint [5] and wood are therefore extracted from literature [24–31] and these will be discussed further below.

Due to the complex structure of wood panel paintings, it is difficult to determine the crack initiation position under an environment-induced cyclic stress. Aurand et al.'s research [32] showed that depending on the wood and ground, the ground layer can be stiffer than the wood just below it, dominating the mechanics at the interace. In this study, cracks were assumed to be initiated in the paint layer because 1) cracks in the paint layer are a precusor to delamination; and 2) the initiation and position of cracks in the paint layer can be visually recorded so the FE simulation results can be compared with DIC measurements on model paintings and the visual observations in the case study paintings. Mecklenburg et al. [5] performed a series of tests on approximately 14-year aged linseed-oil-based paints at 40% to 50% RH and 23 °C. Barbera et al. [7] performed mechanical characterisation of 30-year naturally aged linseed-oil-based paint showing that the linear increase in stiffness for the first ten years is followed by an exponential trend in stiffness thereafter. In addition, Janas et al. [33] recently performed a mechanical characterisation study on 29-year aged linseed-oil-based paints. The results of these studies showed that even after decades of ageing, the mechanical properties of these paints were still changing (becoming stiffer and more brittle). The mechanical behaviour of the paints can be significantly affected by the specific pigments. Brown paint consists of umber pigment or similar earth pigments (many of which are present in the portraits) and cold pressed linseed oil; it has been shown to have the lowest modulus and failure strain of 5 MPa and 1%, respectively [5]. Therefore, it was selected to be the oil paint layer in the FE models and was assumed to be the most fragile part of our case study paintings. To the authors' best knowledge, the fracture toughness of fully aged oil-based paint has not been studied before due to the long ageing process [7]. The fracture energy measured from peel tests of alkyd paint and acrylic gesso was reported as approximately 0.25 N/mm [11]. Considering the fragility of the aged linseed oil paint, a value of 0.025 N/mm was chosen as a reasonable estimate in this study and a parametric study was performed varying the fracture energy to identify its effect on crack initiation time. Varying the fracture energy also allows the study of the impact of the ageing effect on the properties and hence crack initiation. In addition, fully aged paint is not as sensitive to RH changes [5] so the hygroscopic expansion coefficient of the oil paint layer is assumed to be negligible. The Poisson's ratio was taken as 0.3 [14,15].

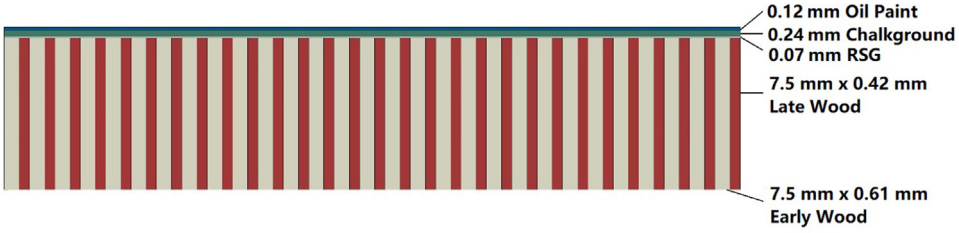

Fig. 1. Typical cross section structure of the Brown Gallery panel paintings exhibited in Knole House. From top to bottom: pigmented oil paint (0.12 mm), chalk ground (0.24 mm), rabbit skin glue (0.07 mm), wood (7.5 mm).

Table 1
Mechanical and hygroscopic expansion properties of RSG (1:5) and Chalk ground (Tested at RH = 70%, 20 °C, 0.5 mm/min).

	Young's Modulus, E (MPa)	Poisson's Ratio, ν	Hygroscopic Expansion Coefficient, q (%/%RH)
RSG (1:5)	2100 ± 200	0.3	0.0681 [1]
Chalk ground	760 ± 50	0.3	0.0159 [1]

The dried RSG and powdered chalk ("Whiting") was supplied by Cornelissen & Son. The RSG was prepared from one part of RSG and five parts of water by weight (1:5). It was left to swell then heated to 40 °C and stirred, followed by cooling to a thick pouring consistency. The chalk ground layer was prepared (1:1) by weight from the warm RSG and powdered chalk, stirred and left to cool. These samples follow the typical concentrations used to make up RSG size and RSG-chalk as the gesso layer for a northern panel. To obtain the mechanical properties of the RSG and chalk ground layers, the following procedure was used to cast the two materials as free films with a rectangular shape. A polyester sheet was used as a sample carrier with electrical insulation tape of thickness 0.12 mm as an approximate thickness gauge to control the thickness of the specimens. The final thicknesses measured using a Vernier calliper were 0.13 mm and 0.5 mm for RSG films and chalk ground films, respectively. The films were then cut to a size of 6 mm in width, 84 mm in length and a gauge length of 56 mm. Tensile tests were performed using an Instron 5544 single-column universal testing machine equipped with a 100 N load cell at 20 °C and 70% RH at a crosshead speed of 0.5 mm/min, chosen to represent the low strain rate at which historical panels move or are subjected to during conservation treatments. The 70% RH was chosen as it was close to the average of 65.2% RH during the period of 1605 – 2015 [18]. The mechanical properties of RSG and chalk ground, namely the Young's modulus and Poisson's ratio, are summarised in Table 1, respectively. The materials are assumed to be isotropic and linear elastic. The average Young's modulus was calculated in the initial linear region of the stress/strain curves for six samples of RSG (0 - 0.014 strain range) and four samples of chalk ground (0- 0.001 strain range) respectively (this excluded any samples that had broken at the grips). The hygroscopic expansion coefficients, q, were taken from Mecklenburg et al. [1] who determined the q values of RSG and "gesso" (at a Pigment Volume Concentration (PVC) of 58.3%) as a function of RH. The values shown in Table 1 are averaged across the tested RH range (3% - 100%).

Note that the PVC of the chalk ground was not measured. Based on a comparison of the measured modulus of 760 MPa with literature, it is probably lower than the PVC values of 85% - 95% in studies of chalk based "gesso" made according to some historical recipes for gilding and paintings [3,34,35]. The Poisson's ratio for "gesso" at such high PVC has also been reported as 0.2 [4]. Due to the relatively low PVC here, the assumed value of 0.3 for the chalk ground is reasonable.

As shown in a report by Ian Tyers for the Brown Gallery paintings [17], the panels are constructed from oak from the Baltic region felled in the early 1600′s. However, "Baltic" oak is not an official species category. In this study, the bulk properties of common oak (Quercus Robur) are extracted from literature and quoted at approximately 50% - 65% RH and 20 °C (ambient conditions) [24–31]. They are summarised as averages of these literature values in Table 2. The FEA model requires the orthotropic elastic properties of earlywood and latewood in the radial (Direction-1), tangential (Direction-2) and longitudinal (Direction-3) directions (see supplementary Fig. 2) and the method to obtain estimates of these from the respective bulk values is outlined below.

A common relationship known as the rule of mixtures (Voigt model) was employed for the radial moduli (E_1), longitudinal moduli (E_3) and transverse Poisson's ratios (ν_{12}) as shown below:

$$X_{bulk} = V_l X^l + V_e X^e \tag{1}$$

Table 2
Elastic and hygroscopic expansion properties of early and latewood in typical oak panels.

Property	Bulk	Earlywood	Latewood
E_1 (GPa)	2.1	1.8	2.5
E_2 (GPa)	1.2	0.98	1.8
E_3 (GPa)	14	11	17
G_{12} (GPa)	0.46	0.36	0.73
G_{13} (GPa)	1.3	1.0	2.1
G_{23} (GPa)	0.98	0.78	1.6
ν_{12}	0.56	0.48	0.68
ν_{13}	0.064	0.064	0.064
ν_{23}	0.033	0.033	0.033
q_1 (%/%RH)	0.18	0.070	0.29
q_2 (%/%RH)	0.29	0.24	0.35
q_3 (%/%RH)	0.020	0.027	0.013

while the inverse rule of mixtures (Reuss model) was employed for tangential moduli (E_2) and shear moduli (G_{12}, G_{13} and G_{23}):

$$\frac{1}{X_{bulk}} = \left(\frac{V_l}{X^l} + \frac{V_e}{X^e}\right)^{-1} \tag{2}$$

where X_{bulk} is any of the bulk properties shown in Table 2 (with the exception of ν_{13}, ν_{23}, q_1, q_2 and q_3), $X^l$and X^e are the respective latewood and earlywood properties, and $V_l = 0.4$ and $V_e = 0.6$ [22] are the volume fractions of latewood and earlywood, respectively.

A second relationship is needed to allow calculation of X^l and X^e. For the radial moduli (E_1) Eq. (3) by Nairn [22] was used:

$$E_1^l = E_1^e \rho^{1.63} \tag{3}$$

where $\rho = 1.225$ [36] is the ratio of latewood to earlywood density and superscripts (l) and (e) indicate latewood and earlywood properties. Similarly, for the tangential moduli (E_2) the second relationship is [22]:

$$E_2^l = E_2^e \rho^3 \tag{4}$$

For the longitudinal moduli (E_3), the ratio shown below was used from a study by Büyüksarı et al. on oak wood [36]:

$$\frac{E_3^l}{E_3^e} = 1.55 \tag{5}$$

For the transverse shear modulus (G_{12}), Cramer et al. [37] give the ratio as 2.0 for loblolly pine:

$$\frac{G_{12}^l}{G_{12}^e} = 2 \tag{6}$$

The shear modulus for latewood and earlywood in the other two directions (G_{13} and G_{23}) has no effect in a 2D simulation so the values were chosen using the same ratio of 2 in Eq. (6).

For the transverse Poisson's ratio (ν_{12}), the ratio in Eq. (7) below was given by Nairn [22] for Douglas fir and the assumption was made that this ratio is the same for the oak wood:

$$\frac{\nu_{12}^l}{\nu_{12}^e} = 1.42 \tag{7}$$

In addition, since the longitudinal Poisson's ratios (ν_{13} and ν_{23}) only have a small effect in a 2D simulation, the Poisson's ratios for both earlywood and latewood were set equal to the respective bulk values [22].

It is worth noting here that using either the Voigt or the Reuss models do not lead to large differences in the calculated parameters due to the fact that the mechanical properties of the earlywood and latewood are not far apart, unlike the usual cases of engineering composites where these can be orders of magnitude different.

The bulk hygroscopic expansion coefficients of oak wood in the three directions (q_1, q_2 and q_3) were taken from Volkmer et al. [28] and are shown in Table 2. In order to estimate the q values for the earlywood and latewood, the following rule of mixtures (Reuss model) was used:

$$q_{i,\ bulk} = \frac{q_i^l E_i^l V_l + q_i^e E_i^e V_e}{E_i^l V_l + E_i^e V_e} \quad for\ i = 1, 2, 3 \tag{8}$$

Using the data by Derome et al. [38] in their study for spruce, the ratio of q in the radial and tangential directions was:

$$\frac{q_2^l}{q_1^l} = 3.3 \text{for latewood} \tag{9}$$

$$\frac{q_2^e}{q_1^e} = 1.2 \text{for earlywood} \tag{10}$$

It was assumed the same ratios can be used for oak too. Finally, Kretchmann and Cramer [39] reported that on average the longitudinal shrinkage of earlywood was about twice as great as latewood for loblolly pine. The same ratio was assumed for oak in this study, therefore:

$$\frac{q_3^e}{q_3^l} = 2 \tag{11}$$

This completes the estimation of all the values shown in Table 2. It should be noted that all the earlywood and latewood properties shown in Table 2 are not experimental results but reasonable estimates, consistent with literature and with oak wood's bulk properties.

3.2. The irreversible cohesive zone model (ICZM)

The cohesive zone approach [40] is implemented in FEA models for the simulation of the initiation and propagation of cracks. Cohesive elements are placed at the position where the crack is expected to grow. Under a given load, the mechanical response of the cohesive elements obeys the traction-separation law (see Fig. 2). In the standard cohesive zone models, the damage variable, D, only starts to accumulate when the critical effective separation displacement, δ_0, is reached and when the value of D reaches one, the element will be deleted (stiffness is equal to zero). However, in this study, the stress induced by the relative humidity change is very small, so damage would not occur. Therefore, the irreversible cohesive zone model (ICZM) is introduced so the effect of fatigue damage under cyclic RH changes can be simulated.

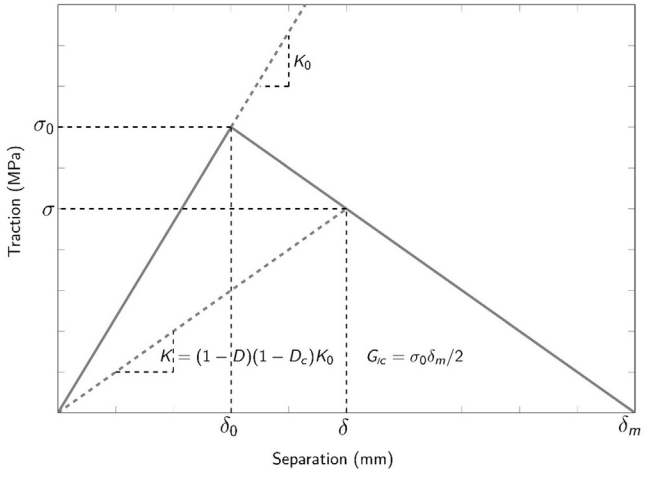

Fig. 2. Traction-separation law used in irreversible cohesive model.

As shown in Fig. 2, a fatigue damage variable, D_c, which will degrade the element stiffness under cyclic loading is introduced [11–13]. When $D_c = 0$, the irreversible traction-separation law is reduced to the standard definition of the traction-separation law and cohesive zone models.

The stress σ in the irreversible cohesive zone model can be calculated using:

$$\sigma = (1 - D)(1 - D_c)K_0\delta \tag{12}$$

where K_0 is the initial stiffness of the elements and δ is the separation displacement. The damage variable D when the element displacement is larger than δ_0 is obtained from:

$$D = \frac{\delta_m(\delta - \delta_0)}{\delta(\delta_m - \delta_0)} \tag{13}$$

where δ_m is the failure separation displacement, and the fatigue damage variable for the current time increment, $D_c(t)$, can be calculated from:

$$D_c(t) = D_c(t - dt) + \Delta D_c \tag{14}$$

where

$$\Delta D_c = \left(\frac{\Delta\delta}{\delta_m - \delta_0}\right)\frac{\sigma}{\sigma_0} \tag{15}$$

$$\Delta\delta = |\delta(t) - \delta(t - dt)| \tag{16}$$

$$\delta(t) = \sqrt{\delta_n^2(t) + \delta_s^2(t) + \delta_t^2(t)} \tag{17}$$

$$\sigma = \sqrt{\sigma_n^2(t) + \sigma_s^2(t) + \sigma_t^2(t)} \tag{18}$$

$$\sigma_n(t) = \sigma_n(t)\mathrm{H}(\delta_n(t)) \tag{19}$$

with the subscripts n, s and t corresponding to the normal, shear and tearing components, respectively. When the models are 2D, the tearing components in the previous equations, σ_t and δ_t, are not included. For mode I loading, fatigue damage only accumulates when the stress is tensile and this is incorporated into Eq. (18) through the Heaviside step function $\mathrm{H}(\delta_n(t))$, whereas shearing and tearing accumulate damage in both positive and negative directions. Therefore, in order to use ICZM, the values of initial interfacial stiffness, K_0, interfacial strength, σ_0, and interfacial fracture energy, G_{IC}, need to be known.

It is important to note that the values of K_0, σ_0, and G_{IC} are not available for 400-year-old oil paints, so a reasonable but arbitrary choice had to be made. As already mentioned in Section 3.1, the G_{IC} of the aged linseed oil paint was taken as 0.025 N/mm. The initial stiffness, K_0, was taken to be 0.2 MPa/mm, which is much lower than the value of 8 MPa/mm used in the models for alkyd paints on canvas [12,13]. The value of the interfacial strength, σ_0, was taken as the strength of the semi-aged umber pigment in linseed oil (0.05 MPa) [5]. The values of damage initiation separation, δ_0, and the final separation, δ_m, can then be calculated accordingly as 0.25 mm and 1 mm, respectively. Note that these values are not measured from experiment, but they are reasonable estimates based on literature. They were used to model both the interfacial and the channelling cracks and were kept the same for both mode I (normal) and mode II (shear) failure modes. The latter are just simplifying assumptions that were necessary due to

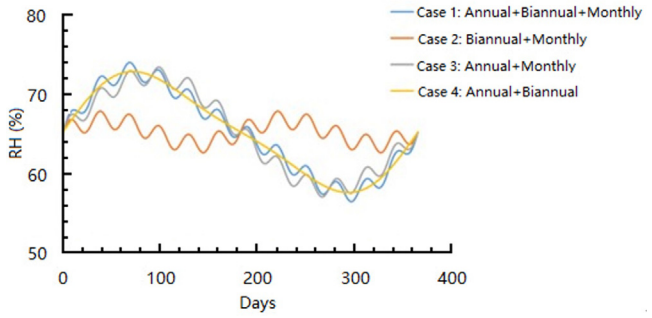

Fig. 3. The RH variation within one year. Case 1 shows the real case with all annual, biannual and monthly variations are combined whereas Cases 2 - 4 show the combinations of just two of these three periodic variations.

the absence of relevant experimental data. It would be interesting, if more experimental data are available in the future, to determine the effect these assumptions have on the estimated crack initiation times. Mixed mode failure analysis was enabled by using a linear mixed mode failure locus [40]. Zhang et al. [13] showed that the change in fracture energy has the most significant effect on the FEA prediction of the crack initiation time in canvas paintings, so a parametric study on fracture energy was also performed.

3.3. Relative humidity cycles

To estimate the crack initiation time in the Brown Gallery panel paintings, the cyclic RH history that the paintings have been exposed to was implemented as a boundary condition in the FE models. The environmental history was obtained using recorded temperature and RH data at the Brown Gallery of Knole House for the period 2000 – 2015 together with Hadley Centre Central England (HadCET) temperature data from 1659. The methodology is detailed in Wood et al. [18] where the historical RH cycles between 1605 and 2015 were reconstructed, showing that the average RH in the Brown Gallery in that period was 65.2%. By performing a Fourier series analysis on the historical RH data, three main amplitudes in the frequency spectrum of the RH cycle were determined: a monthly cycle with an average amplitude of 1.16% RH, a biannual (twice every year) cycle with an average amplitude of 1.51%RH and an annual cycle with an average amplitude of 7.09%RH. These cycles are shown in Fig. 3, assuming each of these three variations follow a sinusoidal form. As shown in Fig. 3, four specific cases will be modelled; Case 1 corresponds to all three variations (annual, biannual and monthly) superimposed to approximate the reconstructed historical data that the wood panels have been exposed to. Cases 2 – 4 are the three possible combinations of including just two of these three variations. These cases were studied in an effort to determine which of these three different cycles (monthly, biannual and annual) are more detrimental to the paintings. Note that Case 2 has a low amplitude and high frequency compared to Case 4 which has a high amplitude and low frequency. Therefore, comparing these cases will allow an investigation of the effects of the frequency and the amplitude of the variation on the possibility of cracking in the painting. This can provide guidelines for optimising the environmental specifications for storing historical wood panel paintings.

3.4. Finite element models

Using the commercial FE software Abaqus [41], the 2D FE models were created for both channelling and interfacial cracks. Both types of cracks can be seen in Supplementary Fig. 3. Channelling cracks typically result in what is known as “tenting” (a), while interlaminar crack result in what is known as “blind cleavage” and “delamination” (b).

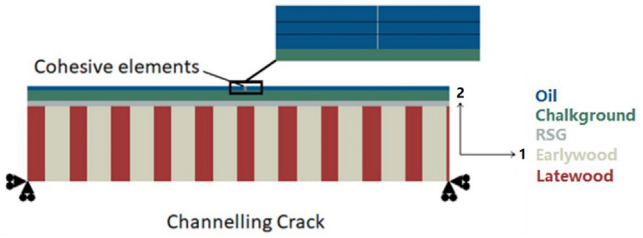

Fig. 4. 2D FE model for channelling crack in a wood panel painting showing the boundary conditions.

Although 2D simulations could lead to a minor overestimation of the crack initiation time [13], the much higher computation time and power consumption of 3D models makes the 2D models a more reasonable choice. All models use 4-node linear 2D plane strain elements (CPE4H) for the linear elastic materials and 2D cohesive elements (COH2D4) are used to represent both the channelling and interfacial cracks.

As mentioned in Section 3.1, it is assumed that the oil paint layer coloured with a raw umber pigment is the most fragile layer in the panel paintings. Therefore, both the channelling and interfacial cracks are assumed to initiate within this layer, i.e., the channelling crack is initiated in the oil paint layer and the delamination interfacial crack is initiated between the oil paint and chalk ground.

Channelling crack

Fig. 4 shows the model for a channelling crack propagation through the oil paint layer and arresting at the oil paint/chalk ground interface. From top to bottom, the oil paint layer, chalk ground layer, RSG layer and wood substrate are modelled with 3, 6, 2 and 40 elements in the 2-direction. To reduce the simulation time, a double-biased mesh was used in the 1-direction with a minimum element size of 0.04 mm at the centre of the model and a maximum element size of 1 mm at both edges, which, through a mesh sensitivity study, was found to provide mesh-independent results. The length of the model is 36 mm, which was estimated to be large enough to eliminate any edge-effects on the model output. For the boundary conditions, only the two bottom corners are restricted from moving in the 1- and 2-directions to allow bending of the panel during the simulation. The RH cycles described in Section 3.3 are applied to the whole model.

Interfacial crack

Fig. 5 shows the FE model geometry for the case representing an interfacial crack propagating between the oil paint and chalk ground layers. The same dimensions are used in both the channelling and interfacial crack models, so the length is again 36 mm. The oil paint layer is modelled with two rows of 600 elements; the chalk ground layer is modelled with four rows of 600 elements; the RSG layer is modelled with one row of 600 elements and the

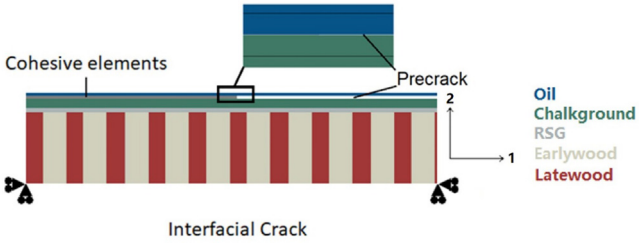

Fig. 5. 2D FE model for an interfacial crack between an oil paint layer and chalk ground layer in a wood panel painting showing the boundary conditions.

wood panel is modelled with sixty rows of 300 elements. This mesh was found to give mesh-independent results. A pre-crack is introduced into the model by inserting a layer of default-thickness cohesive elements along only half the length (18 mm) of the whole model, between the oil paint and chalk ground layer. The length was chosen to eliminate edge-effects. The two bottom corners are fixed in the 1- and 2-direction and the RH cycles are applied to the whole model.

4. Results and discussion

Using the irreversible cohesive zone model described in Section 3.2, the crack initiation time of both the channelling and interfacial cracks was estimated using the 2D FE model, for Cases 1–4 of cyclic RH in Fig. 3. For the interfacial crack, the 2D model can also provide estimates for the crack growth rate. For the case of the channelling crack, this not possible as the crack direction is through the layer of the oil paint which is very thin (only 0.12 mm).

4.1. Crack initiation time

The crack initiation is defined as the point when the value of the damage variable, D_c, reaches one. Table 3 compares the crack initiation time for both channelling and interfacial cracks under the different cases of RH cycles (Cases 1–4 in Fig. 3).

It is seen that the under all RH cycles, the channelling crack initiates slightly earlier than the interfacial crack (except for case 2 where cracks did not initiate after the whole simulation period of 410 years). In addition, as expected, using only two of the three possible cyclic variations (Cases 2 – 4) postpones the initiation of both types of cracks. For case 1 representing the real environmental variation, the channelling and interfacial cracks initiate after approximately 124 and 136 years, respectively. If the environment in which the paintings are displayed and stored is such that the annual variation corresponding to the seasonal changes from winter to summer is prevented (Case 2 in Fig. 3), the initiation of both types of cracks can be postponed significantly to more than 410 years. This corresponds to eliminating the annual variation of the cyclic RH which has the highest amplitude but the lowest frequency of the three cyclic variations.

Due to the low magnitude and frequency of the biannual cycle, its effect on the crack initiation time was not significant when it was omitted from the RH variation (Case 3 in Fig. 3). From Table 3, the initiation times increased to 132 and 144 years, i.e., delaying the crack initiation for roughly a decade with both types of cracks. However, Table 3 shows that if the monthly variations in RH (Case 4 in Fig. 3) can be eliminated, this can extend the crack initiation time by more than a century. Note that the monthly variation is a cycle with a low magnitude but a high frequency. Therefore, the results of the study imply that both magnitude and frequency of the cyclic RH are important, with the amplitude being potentially more serious than the frequency in terms of possible damage in the panel painting. This agrees with Paris et al. [42], specifically that the amplitude of a cyclic load needs to reach a threshold before cracks can initiate.

Table 3
Comparison of crack initiation time for channelling and interfacial cracks under different RH cycles (Cases 1–4 as shown in Fig. 3).

RH Cycle	Crack initiation time (Years)	
	Channelling	Interfacial
Case 1	124	136
Case 2	>410	>410
Case 3	132	144
Case 4	227	245

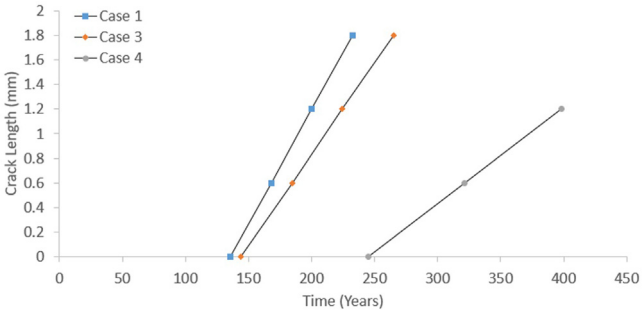

Fig. 6. Interfacial crack length versus time under different RH cycles (cases 1, 3 and 4 as shown in Fig. 5). Note the data for the RH cycle without the annual variation (case 2) is not shown here because the crack had not initiated by the end of the simulation period (410 years).

Tantideeravit et al. [11] and Zhang et al. [13] reported times to crack initiation using a similar model to this study but for an alkyd paint on primed canvas. Though it is hard to compare the two studies as the materials, the geometry and RH cycles were all different, the time to crack initiation there for a RH cycle varying from 45%RH to 55% RH was approximately 90 years. Interestingly, that is not vastly dissimilar to the times reported in the current study for Cases 1, 3 and 4 (see Table 3) which included the annual RH cycle 65.2 ± 7.09% RH. Note that a big difference in the two studies is that the alkyd paint was modelled as a viscoelastic material with a very low dimensionless equilibrium modulus ($g_\infty = 0.01$) compared to the linear elastic moduli here, though the energy release rate for the alkyd paint was much higher at 0.25 N/mm, compared to 0.025 N/mm used in the current study.

4.2. Crack growth rate

Besides the crack initiation time, the 2D model also provides prediction of the crack growth rate for the case of the interfacial crack. Fig. 6 compares the crack growth rate of interfacial crack under the different RH cycles (cases 1, 3 and 4 in Fig. 3). As expected, a more stable environment can postpone the crack initiation and decrease the crack growth rate at the same time. The average times for the interfacial crack to grow 0.6 mm (3 elements) under case 1, 3 and 4 RH cycles are approximately 30, 40 and 80 years, respectively. These results will be compared to experimental testing taking place at present on artificially aged reconstruction samples as part of the wider research.

In conclusion, when storing and exhibiting historical panel paintings, controlling the RH to eliminate the annual RH variation (case 2) will help keep the paintings in a good state of preservation. But if a painting is extremely fragile, a more tightly controlled environment is required to eliminate the biannual and monthly variations [14,15]. This is very important where new cracks have initiated in historical panels as the crack propagation results in Fig. 6 show.

4.3. Parametric study on the fracture energy

As stated in Section 3.2, the same traction-separation law was assumed for both channelling and interfacial cracks. As fracture data is unavailable for the cohesive strength, σ_0, and the fracture energy, G_{IC}, for either the oil paint or the oil paint/chalk ground interface, a parametric study was performed by varying the fracture energy, G_{IC}, while maintaining the same initial stiffness, K_0, and displacement at damage initiation, δ_0. Note that this implies that

Table 4
Effect of fracture energy, G_{IC}, on the initiation time predictions for channelling and interfacial cracks under the historical ambient RH cycle (case 1 in Fig. 3).

Fracture energy, G_{IC} (N/mm)	Crack initiation time (Years)	
	Channelling crack	Interfacial crack
0.0125	63	68
0.025	124	136
0.05	225	271

the cohesive stress, σ_0, is also kept constant, whilst δ_m increased as G_{IC} is increased.

The estimates for the crack initiation time corresponding to G_{IC} values of 0.0125, 0.025 and 0.05 N/mm under the reconstructed RH cycle (Case 1 in Fig. 3) are compared in Table 4. It is seen that the initiation time varies approximately linearly with the G_{IC}, with a higher G_{IC} postponing the crack initiation as expected. The initiation time for the G_{IC} value of 0.0125 N/mm is around 63 years. The National Trust conservation team responsible for the these paintings at Knole House believe that these values are realistic, as it is thought that cracks were formed within the first few decades of the paintings being displayed [43]. It is worth pointing out the possible limitations of the models used here in that, in reality, the crack initiation is affected by not only the cyclic change in RH, but also "single event" very high or low changes in RH, a large change in temperature and external stresses induced by historical additions to the panels or moving the paintings within Knole House or for loans. In addition, because of the complexity of the wood panel painting, the model needs a large number of material parameters (see all the data listed in Tables 1 and 2), and several of these were estimated rather than directly measured through experiments. Therefore, accurate measurements need to be performed to obtain the material properties where possible and crucially the actual fracture properties of the fully aged oil paints, even though the latter is of course highly challenging for the reasons explained in Section 3.1.

5. Conclusions

Finite element models have been used to compare the initiation time of channelling and interfacial cracks under various RH cycles, including the reconstructed environmental history that the panel paintings in the Brown Gallery at Knole House have been exposed to for the period of 1605 - 2015. It is seen that a channelling crack initiates slightly earlier than an interfacial crack. As expected, controlled RH can postpone the initiation of both the channelling and interfacial cracks. RH cycles with larger variation seems to be the dominant cause of the initiation of cracks in the paint layer, i.e., controlling the RH environment against annual variations from winter to summer seasons is shown to significantly extend the crack initiation of the panel paintings. This agrees with the authors' research on alkyd on canvas paintings [11,13] and Paris et al. [42]. However, for more fragile or valuable paintings, a more tightly controlled environment that will eliminate lower amplitude but higher frequency RH variations than the annual variations can be a good preventive conservation strategy.

Estimating the cracking behaviour in paintings is a challenge as there are many parameters that need to be taken into consideration. In this work, the effect of changing RH is studied but other variables such as RH and temperature dependence of mechanical properties, temperature variation, the ageing process of each component of the panel painting and the non-uniform thickness of each layer of the painting can all be investigated in the future with the developed model. Furthermore, the possibility of cracking initiating in other layers such as the chalk ground can also be studied. Although this work is an initial attempt, FE models have shown great potential in providing information towards optimising the display and storage environment of historical panel paintings.

Acknowledgments

The funding for this project was provided by the Engineering and Physical Sciences Research Council (EPSRC) with grant references EP/P0024391/1 and EP/P003613/1. We would also like to acknowledge Cecilia Gauvin, Joseph Wood and Edric Yi Zhe Low who helped with this research at various stages of the project.

Supplementary materials

Supplementary material associated with this article can be found, in the online version, at doi:10.1016/j.culher.2023.02.007.

References

[1] M.F. Mecklenburg, C.S. Tumosa, W.D. Erhardt, Structural response of painted wood surfaces to changes in ambient relative humidity, Paint. Wood Hist. Conserv. (1998) 464–483.
[2] G. Thomson, The Museum Environment, 2nd ed., Elsevier, Cornwall, 2013.
[3] Ł. Bratasz, K.G. Akoglu, P. Kékicheff, Fracture saturation in paintings makes them less vulnerable to environmental variations in museums, Herit. Sci. 8 (2020) 1–12.
[4] B. Rachwał, Ł. Bratasz, L. Krzemień, M. Łukomski, R. Kozłowski, Fatigue damage of the gesso layer in panel paintings subjected to changing climate conditions, Strain 48 (2012) 474–481.
[5] M.F. Mecklenburg, C.S. Tumosa, D. Erhardt, The changing mechanical properties of aging oil paints, MRS Online Proc. Libr. Arch. (2004) 852.
[6] Ł. Bratasz, M.R.Vaziri Sereshk, Crack saturation as a mechanism of acclimatization of panel paintings to unstable environments, Stud. Conserv. 63 (2018) 22–27.
[7] D. Barbera, C. Young, M. Charalambides, A.C. Taylor, R. Zhang, A methodology for the use of alkyd paint in thermally aged easel painting reconstructions for mechanical testing, J. Cult. Herit. 55 (2022) 237–244.
[8] F. Giorgiutti-Dauphiné, L. Pauchard, Painting cracks: a way to investigate the pictorial matter, J. Appl. Phys. 120 (2016) 065107.
[9] C. Young, The painted surface and interface, in: N. Kos, P. van Duin, A. Kruse (Eds.), The conservation of panel paintings and related objects: research agenda 2014-2020, Netherlands Organisation for Scientific Research: The Hague, NWO, 2014.
[10] L. Krzemień, M. Łukomski, Ł. Bratasz, R. Kozłowski, M.F. Mecklenburg, Mechanism of craquelure pattern formation on panel paintings, Stud. Conserv. 61 (2016) 324–330.
[11] S. Tantideeravit, M. Charalambides, D. Balint, C. Young, Prediction of delamination in multilayer artist paints under low amplitude fatigue loading, Eng. Fract. Mech. 112 (2013) 41–57.
[12] J.D. Wood, C. Gauvin, C.R. Young, A.C. Taylor, D.S. Balint, M.N. Charalambides, Cracking in paintings due to relative humidity cycles, Procedia Struct. Integr. 13 (2018) 379–384.
[13] R. Zhang, J. Wood, C. Young, A. Taylor, D. Balint, M. Charalambides, A numerical investigation of interfacial and channelling crack growth rates under low-cycle fatigue in bi-layer materials relevant to cultural heritage, J. Cult. Herit. (2021).
[14] E. Bosco, A.S. Suiker, N. Fleck, Crack channelling mechanisms in brittle coating systems under moisture or temperature gradients, Int. J. Fract. 225 (2020) 1–30.
[15] E. Bosco, A.S. Suiker, N.A. Fleck, Moisture-induced cracking in a flexural bilayer with application to historical paintings, Theor. Appl. Fract. Mech. 112 (2021) 102779.
[16] K. Roe, T. Siegmund, An irreversible cohesive zone model for interface fatigue crack growth simulation, Eng. Fract. Mech. 70 (2003) 209–232.
[17] D. Jaskierny, The classification and categorisation of crack patterns and delamination found on panels in the brown gallery of knole house (Postgraduate Diploma Thesis), in: University of London, London, 2017.
[18] J.D. Wood, C. Gauvin, C.R. Young, A.C. Taylor, D.S. Balint, M.N. Charalambides, Reconstruction of historical temperature and relative humidity cycles within Knole House, Kent, J. Cult. Herit. 39 (2019) 212–220.
[19] J.v.d. Berg, Analytical chemical studies on traditional linseed oil paints (PhD Thesis), in: swammerdam Institute for Life Sciences (SILS), Amsterdam, 2002.
[20] J. Alexander, Glue and gelatin, Chemical Catalog Company, Incorporated, London, 1923.
[21] A.P. Schniewind, J. Barrett, Wood as a linear orthotropic viscoelastic material, Wood Sci. Technol. 6 (1972) 43–57.
[22] J.A. Nairn, A numerical study of the transverse modulus of wood as a function of grain orientation and properties, Holzforschung 61 (2007) 406–413.
[23] T.K. Bader, K. de Borst, K. Fackler, T. Ters, S. Braovac, A nano to macroscale study on structure-mechanics relationships of archaeological oak, J. Cult. Herit. 14 (2013) 377–388.

[24] A. Vorobyev, O. Arnould, D. Laux, R. Longo, N.P. van Dijk, E.K. Gamstedt, Characterisation of cubic oak specimens from the Vasa ship and recent wood by means of quasi-static loading and resonance ultrasound spectroscopy (RUS), Holzforschung 70 (2016) 457–465.
[25] R.F.S. Hearmon, The elasticity of wood and plywood, Forest Products Research, Special Report 7 (1948) Part 1.
[26] C. Preziosa, Méthode De Détermination Des Constantes élastiques du Matériau Bois Par Utilisation Des Ultrasons (PhD Thesis), Université d'Orléans, Orléans-France, 1982.
[27] J. Bodig, B.A. Jayne, Mechanics of Wood and Wood Composites, Van Nostrand Reinhold, New York, 1982.
[28] T. Volkmer, T. Lorenz, P. Hass, P. Niemz, Influence of heat pressure steaming (HPS) on the mechanical and physical properties of common oak wood, Eur. J. Wood Wood Prod. 72 (2014) 249–259.
[29] K. de Borst, T.K. Bader, C. Wikete, Microstructure–stiffness relationships of ten European and tropical hardwood species, J. Struct. Biol. 177 (2012) 532–542.
[30] T.K. Bader, J. Eberhardsteiner, K. de Borst, Shear stiffness and its relation to the microstructure of 10 European and tropical hardwood species, Wood Mater. Sci. Eng. 12 (2017) 82–91.
[31] M. Khelifa, A. Khennane, Numerical analysis of the cutting forces in timber, J. Eng. Mech. 140 (2014) 523–530.
[32] A. Aurand, C. Gauvin, D. Jullien, C. Young, Understanding the moisture induced fatigue damage in panel paintings: a methodological approach for quantifying the role of preparatory layers in the overall response, in: ICOM-CC Joint Interim Meeting. Physical issues in the conservation of Paintings: Monitoring, Documenting and Treatment, 2016.
[33] A. Janas, M.F. Mecklenburg, L. Fuster-López, R. Kozłowski, P. Kékicheff, D. Favier, C.K. Andersen, M. Scharff, Ł. Bratasz, Shrinkage and mechanical properties of drying oil paints, Herit. Sci. 10 (2022) 181.
[34] S. Michalski, D. Bigelow, Crack Mechanisms in Gilding, Gilded Wood, Sound View Press, Madison, 1991.
[35] M.F. Mecklenburg, Some mechanical and physical properties of gilding gesso, Gilded Wood Conservation and History D. Bigelow, E. Cornu, G.J. Landrey and C. van Horne (Eds), Sound View Press, Madison, 1991.
[36] Ü. Büyüksarı, N. As, T. Dündar, Intra-ring properties of earlywood and latewood sections of sessile oak (Quercus petraea) wood, Bioresources 13 (2018) 836–845.
[37] S. Cramer, D. Kretschmann, R. Lakes, T. Schmidt, Earlywood and latewood elastic properties in loblolly pine, Holzforschung 59 (2005) 531–538.
[38] D. Derome, A. Rafsanjani, S. Hering, M. Dressler, A. Patera, C. Lanvermann, M. Sedighi-Gilani, F.K. Wittel, P. Niemz, J. Carmeliet, The role of water in the behavior of wood, J. Build. Phys. 36 (2013) 398–421.
[39] D.E. Kretschmann, S.M. Cramer, The role of earlywood and latewood properties on dimensional stability of loblolly pine, in: Proceedings of the Compromised Wood Workshop, 2007, pp. 215–236. 2007 January 29-30. Christchurch, NZ: Wood Technology Research Centre, School of Forestry, University of Canterburypages2007.
[40] Cohesive elements, in: Abaqus Analysis User's Guide, Dassault Systèmes, Vélizy-Villacoublay, France.
[41] Abaqus, in, Dassault Systèmes, Vélizy-Villacoublay, France (2023).
[42] P. Paris, F. Erdogan, A critical analysis of crack propagation laws, J. Basic Eng. 85 (4) (1963) 528–533.
[43] N. Blade, R. Helen, Personal communation, in, 2021.